Materials Science and Engineering C 33 (2013) 1702–1709

Contents lists available at SciVerse ScienceDirect

Materials Science and Engineering C

journal homepage: www.elsevier.com/locate/msec

Preparation of novel carbon microfiber/carbon nanofiber-dispersed polyvinyl alcohol-based nanocomposite material for lithium-ion electrolyte battery separator

Ajit K. Sharma [a], Prateek Khare [a], Jayant K. Singh [a,*], Nishith Verma [a,b,**]

[a] Department of Chemical Engineering, Indian Institute of Technology Kanpur, Kanpur 208016, India
[b] Center for Environmental Science and Engineering, Indian Institute of Technology Kanpur, Kanpur 208016, India

ARTICLE INFO

Article history:
Received 4 March 2012
Received in revised form 3 November 2012
Accepted 26 December 2012
Available online 31 December 2012

Keywords:
Li-ion battery separator
Polyvinyl alcohol
Carbon micro-nanofibers
Suspension polymerization
Ionic conductivity

ABSTRACT

A novel nanocomposite polyvinyl alcohol precursor-based material dispersed with the web of carbon microfibers and carbon nanofibers is developed as lithium (Li)-ion electrolyte battery separator. The primary synthesis steps of the separator material consist of esterification of polyvinyl acetate to produce polyvinyl alcohol gel, ball-milling of the surfactant dispersed carbon micro-nanofibers, mixing of the milled micron size (~500 nm) fibers to the reactant mixture at the incipience of the polyvinyl alcohol gel formation, and the mixing of hydrophobic reagents along with polyethylene glycol as a plasticizer, to produce a thin film of ~25 μm. The produced film, uniformly dispersed with carbon micro-nanofibers, has dramatically improved performance as a battery separator, with the ion conductivity of the electrolytes ($LiPF_6$) saturated film measured as 0.119 S-cm^{-1}, approximately two orders of magnitude higher than that of polyvinyl alcohol. The other primary characteristics of the produced film, such as tensile strength, contact angle, and thermal stability, are also found to be superior to the materials made of other precursors, including polypropylene and polyethylene, discussed in the literature. The method of producing the films in this study is novel, simple, environmentally benign, and economically viable.

1. Introduction

Lithium-ion battery has an anode and a cathode separated by a thin microporous film made of a polymeric or an inorganic material, also known as separator. The role of the separator is to keep the positive and negative electrodes separated. It prevents internal short-circuiting and simultaneously permits the transport of the ionic charge carriers. It must be chemically and electrochemically stable toward the electrolytes, in particular during the battery operation. As the electrodes and separator are wound together during the battery assembling, the separator must be mechanically strong to withstand the induced high tension; otherwise, there is a risk of short-circuiting in the battery during the operation. In addition, the separator material should be thin and should have relatively small electrical resistivity or large ion conductivity, good electrolyte wettability, and thermal stability [1,2]. The last but not the least, the material should be inexpensive. In general, it is extremely difficult and challenging to develop such materials.

Polyethylene (PE) and polypropylene (PP) are two common precursors used for preparing separators for Li-ion batteries. The PE and PP separators have good tensile strength and are electrochemically stable toward the electrolyte and electrode materials, preventing internal short-circuiting or rapid overcharging of the battery. One of the major drawbacks of such separators is relatively poor compatibility with liquid electrolytes because of their hydrophobic property. Another major drawback is the high manufacturing cost of PE and PP [3,4].

Many studies have been performed for modifying the PE and PP separator materials using various methods, such as coating them with gel electrolytes [5] and polymeric nanoparticles [6]; SiO_2 deposition [7]; and grafting with acrylic acid and diethyleneglycol–dimethacrylate [8], methyl methacrylate [9] and polyacrylate [10], and with siloxane using electron beam irradiation [11]. A PP-PE composite modified by the electrospun polyacrylonitrile (PAN) nanofibers also has been prepared [12]. Such modified separators exhibit relatively superior mechanical strength and compatibility with the liquid electrolyte, although the manufacturing cost of the modified PE- and PP-based separators is high.

The studies on the development of Li-ion battery separators made of non-PP- and non-PE-based precursors are few. Kuribayashi [13] developed a cellulose precursor-based composite material by incorporating fine fibrillia cellulosic fibers in a microporous cellulosic film. The PVdF–HFP precursor-based separators with or without reinforcement with suitable inorganic fillers have also been prepared [14,15]. However, such materials are relatively expensive.

Polyvinyl alcohol (PVA) is a relatively low-cost and environmentally benign material. PVA has been used as an electrolyte in Li-ion battery [16]. It also has been used as a separator, in alkaline battery applications [17,18] and also for zinc electrode-based cells [19]. To our knowledge, PVA has not been used as a precursor for the battery

* Corresponding author. Tel.: +91 512 2596124; fax: +91 512 2590104.
** Correspondence to: N. Verma, Department of Chemical Engineering, Indian Institute of Technology Kanpur, Kanpur 208016, India. Tel.: +91 512 2596124; fax: +91 512 2590104.
E-mail addresses: jayantks@iitk.ac.in (J.K. Singh), nishith@iitk.ac.in (N. Verma).

0928-4931/$ – see front matter © 2012 Elsevier B.V. All rights reserved.
http://dx.doi.org/10.1016/j.msec.2012.12.083

separator material, except in [20]. However, in that study, no characterization data for the performance evaluation are reported.

In this study, a simple, economically viable method of developing a novel PVA-based thin polymeric film, in situ dispersed with the hierarchical web of carbon microfibers (ACFs) and carbon nanofibers (CNFs) during a polymerization stage, is experimentally demonstrated, as a potential Li-ion electrolyte battery separator. PVA exhibits high abrasion resistance, elongation, tensile strength, and flexibility [16]. Carbon nanotubes (CNTs) have been used as potential additives to polymers because of their excellent mechanical and electrical properties [21,22]. Similarly, the web of ACF/CNF developed as adsorbents has demonstrated excellent chemical resistance in both gaseous and aqueous phases [23–25]. Therefore, ACF/CNF dispersed within the polymeric matrix of PVA is a potential candidate for battery separator material. In this study, different requisite properties of the separator were imparted to the material at different stages of the synthesis. The novelty of the study was to produce an in situ dispersion comprising a ball-milled hierarchical (the order of two scales, micrometer, and nanometer) structure of ACF/CNF using a surfactant, which is compatible with a standard reactant mixture used for the production of PVA by esterification. Such ACF/CNF/PVA nanocomposite materials had enhanced mechanical strength, large ionic conductivity, and electrolyte wettability, which are superior to or comparable with the reported literature data.

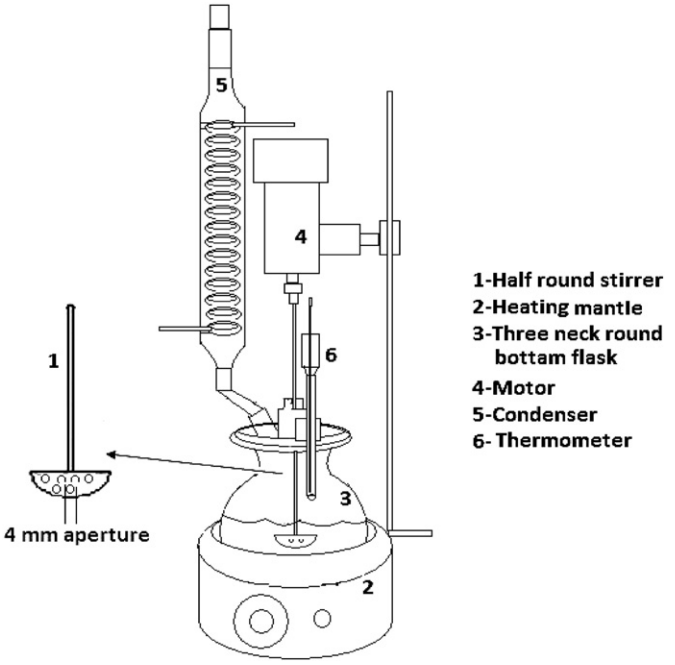

Fig. 1. Schematic of reaction-assembly for the synthesis of polymeric films.

2. Materials and methods

2.1. Reagents

Polyvinyl acetate (PVAc) (degree of polymerization = ~1168) was purchased from Sigma Aldrich (Germany). Methanol, methyl acetate, sodium hydroxide, and sodium dodecyl sulfate (SDS) were purchased from s.d. fine-Chem. ltd., India. Methyl acrylate, acrylonitrile, potassium persulfate, polyethylene glycol (PEG), and $LiPF_6$ were purchased from Merck (Germany). All reagents were of analytical grade with high purity. The hierarchical web of ACF/CNF was synthesized separately as per the procedure described in [23–25].

2.2. Synthesis

The synthesis primarily consisted of the following four steps: (1) a gel of PVA was produced by the esterification of PVAc. Degree of hydrolysis of synthesized PVA was experimentally found to be 92–94%, as per the method described in the literature [26]. (2) Samples of ACFs/CNFs dispersed in SDS, used as the surfactant, were ball-milled to produce a suspension of micron size (~500 nm) ACF/CNF. (3) The produced suspension was added to the reactant mixture of step (1) at the incipience of the PVA gel formation, and (4) acrylonitrile and methyl acrylate as hydrophobic reagents and PEG as a plasticizer were added to produce the slurry-like composite material of ACF/CNF/PVA. Thereafter, the slurry was coated on a Teflon sheet to produce a thin film of ~25 μm thickness for the end application.

Fig. 1 shows the experimental setup used for the synthesis of ACF/CNF/PVA gel by esterification. A 2-l-3-neck round-bottom flask was used for esterification. The flask was attached with a heating mantel and a reflux condenser. A specifically designed half-round mechanical stirrer was used for mixing the reactant mixture. The stirrer perforated with 4-mm holes created homogeneity in the reactant solution and prevented agglomeration of the fibers. The reflux condensing water in the reflux-condenser ensured a constant level of the solution in the flask.

A mixture of 62% (w/w) PVAc in 99% (w/w) methanol was stirred in a separate container to prepare a homogeneous solution. The temperature of the assembly was maintained constant at 60 °C. To this solution, 25 ml of methanol and 22 ml of methyl acetate were added. The solution was mixed using the stirrer at the speed of 130 rpm till a transparent solution was obtained. To this solution, 5 ml of methanolic sodium hydroxide (2.5% of NaOH in methanol) was added. After approximately 15 min, the gel formation started. At the incipience of the gel formation, the ball-milled hierarchical web of ACF/CNF prepared separately in SDS was added to the reactant mixture.

Approximately 0.1 g of the ACF/CNF composite material was randomly cut into small pieces (~1 mm) and added into 20 ml of SDS-water (0.5%, w/w) solution. The solution was transferred to a nanoball mill (Retsch Planetary Ball Mill PM100, Germany) and milled for 2 h at 150 rpm, using 10 mm W-balls (25 in number). This solution containing micron nanofibers (~500 nm) was subsequently transferred to the reactant mixture for esterification, discussed in the preceding paragraph. Some samples of ACF/CNF were also ball-milled using methanol as a solvent instead of SDS to disperse the composite. Further, in order to ascertain the effect of time of ball-milling on the size of the fibers produced, the SDS-dispersed samples were ball-milled for different times (15 min, 60 min, 120 min, 240 min). As discussed later in the manuscript, the film incorporated with the ACF/CNF composite dispersed in SDS and ball-milled for 2 h performed superior to the other samples.

After approximately 45 min of adding the ball-milled ACF/CNF to the mixture, a black gel-like structure was obtained. Next, 100 ml of Milli-Q water was added. The temperature and the stirrer speed were increased to 80 °C and 150 rpm, respectively. After approximately 2 h, a black solution was obtained. The temperature of the solution was decreased to 60 °C. To this solution, 5 ml of methyl acrylate, 10 ml of acrylonitrile, and 0.1 g of potassium persulfate as the initiator were sequentially added. After approximately 6 h, the black solution turned into whitish (milky) black. The heater was switched off. When the temperature reached the room temperature (~30 °C), 30 ml of PEG was added to the produced solution. After approximately 3 h, black slurry-like material was obtained. The stirrer was stopped, and the slurry was removed and cast on a Teflon sheet using a thin film applicator. Next, the cast material was vacuum dried (~1 mTorr) for 72 h in an oven at 110 °C before using it for the surface characterization and the performance evaluation study.

Fig. 2 shows the process flow sheet for the synthesis of the ACF/CNF-dispersed PVA nanocomposite material. In this paper, the different prepared materials are labeled as PVA-M, PVA-S-BM-CNF, and PVA-SL-BM-CNF for reference purposes, depending on the types of

reagents used and the methods. PVA-M represents the PVA-based separator film prepared by incorporating hydrophobic monomers (acrylonitrile and methyl acrylate) without ACF/CNF. PVA-S-BM-CNF represents the film prepared by dispersing ball-milled ACF/CNF in SDS, whereas PVA-SL-BM-CNF represents the film prepared by dispersing ball-milled ACF/CNF in methanol. All materials were prepared in triplicates for the reproducibility of their properties discussed in the next sections.

2.3. Performance evaluation

The ACF/CNF/PVA composite film prepared as a battery separator was characterized for the electrolyte-ion conductivity, contact angle, tensile strength, surface functional groups, thermal stability, air permeability and mean pore size. The surface morphology of the samples was studied using the Supra 40 VP Field Emission scanning electron microscopy (SEM) procured from Zeiss, Germany. All images were captured with VPSE detector at the accelerating voltage of 20 kV and filament current of 2.37 A at a working distance of 6–7 mm. The resistivity or ionic conductivity was measured by an I-V source meter (Keithley 6221, USA). The tensile strength was measured by a tensile machine (UTM-Zwick/roell-Z010, Germany). The electrolyte wettability was ascertained by measuring the contact angle using the goniometer (Rame-hart-200, Germany). Infrared (IR) spectrum of the samples was obtained using FTIR spectrophotometer (Tensor 27, Brucker, Germany). The spectra were taken on the attenuated total reflectance (ATR) mode using Ge crystal, over wave numbers ranging between 400 and 4000 cm^{-1}. Differential scanning calorimetry (DSC) analysis (Toledo-Mettler, USA) was carried out to ascertain the thermal stability over the temperature range between 30 °C and 350 °C. The film thickness was measured by an optics-based thin-film measurement system (Filmetrix, US). Air permeability and the mean pore size were determined using the automated gas permeability measurement instrument (model no. CCF-20-A, PMI, Porous Materials, Inc., USA).

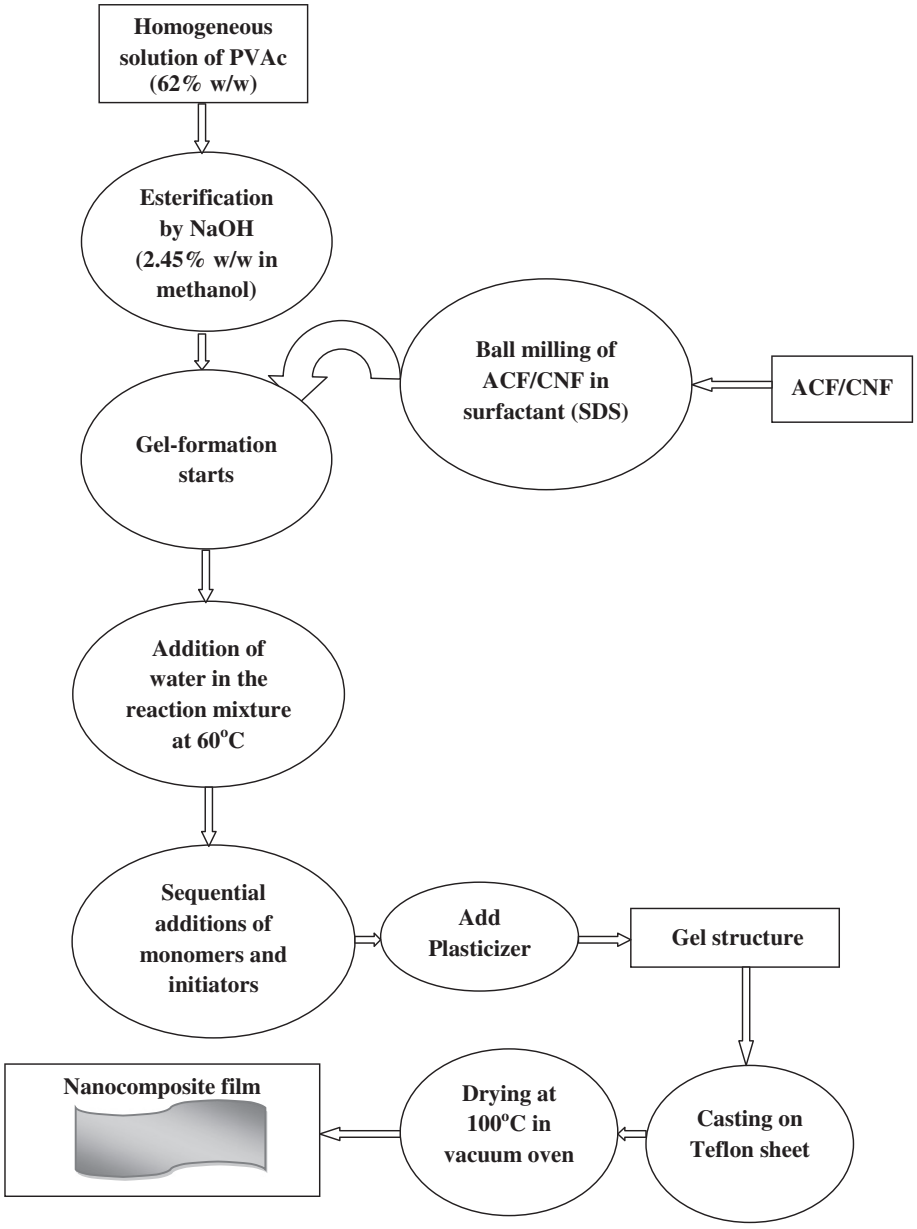

Fig. 2. Process flow sheet for separator material synthesis.

3. Results and discussion

3.1. Surface morphology

The surface morphology of the prepared material was investigated using the SEM images. Fig. 3 shows the images of PVA-M and PVA-S-BM-CNF films. The images are shown at low (100 and 500X) and high (10KX) magnifications for both materials. As observed from Fig. 3A for PVA-M and Fig. 3B for PVA-S-BM-CNF, both materials are porous. However, the external surface of PVA-S-BM-CNF is observed to be rough when compared with the PVA-M film. As also observed from the images shown in Fig. 3A-2 and B-2, the number of pores or pores-content has considerably increased in PVA-S-BM-CNF when compared with its counterpart PVA-M. As shown later, the enhanced pores content is favorable for the absorbability of the electrolytes and high ionic conductivity. Fig. 3A-3 and B-3 shows the corresponding images at higher magnifications. There are two salient observations: (1) The average size of most of the pores in PVA-S-BM-CNF is below 1 μm. (2) The ACF/CNF particles with submicron length and nanometer diameter are dispersed within the film. The important feature of the film is that the dispersed fibers were embedded within the polymeric films along the film surface and not transversely protruded outside the external surface. As discussed later, dispersion of ACF/CNF within the film was responsible for increased mechanical strength, wettability, and ion conductivity.

The mean pore size and air permeability were determined using the automated gas permeability measurement instrument (Model No. CCF-20-A, PMI, Porous Materials, Inc., USA). The mean pore size of PVA-M and PVA-S-BM-CNF were measured to be approximately 228 nm and 180 nm, respectively. The corresponding Darcy permeability constant was measured to be 41×10^{-5} and 27×10^{-5}, respectively. Therefore, the addition of CNFs in the polymeric matrix results in a decrease in the mean pore size and the permeability constant. The numerical value of the mean pore size obtained for the synthesized

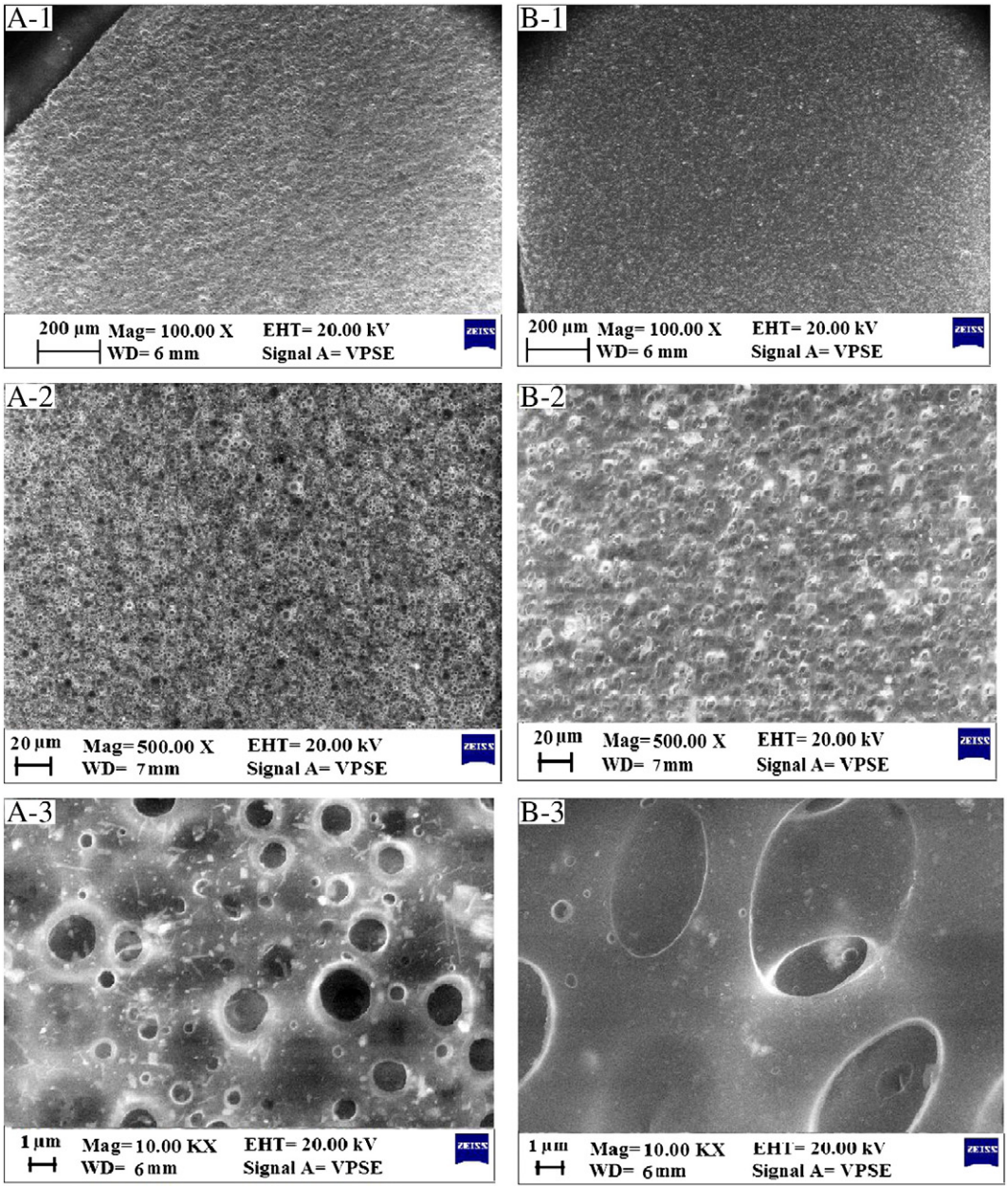

Fig. 3. SEM analysis of PVA-M (A) and PVA-S-BM-CNF (B) membrane at low (100X (A-1, B-1) & 500X (A-2, B-2)) and higher (10KX (A-3, B-3)) magnification.

material in this study is within the order of magnitude of the data reported in the literature for the PVdF and PE precursors-based Li-ion battery separators [27]. Also, Arora et al. [1] have recommended pore diameter<1 μm or 1000 nm for such batteries. Further, Lee et al. [28,29] have experimentally measured the permeability constant of 2×10^{-5} or greater for PE-based battery separators.

As mentioned earlier, some samples (PVA-SL-BM-CNF) were prepared without using the surfactant (SDS), in which case ACFs/CNFs were dispersed in methanol, the reagent used as a solvent for esterification. However, for such materials, the pores were found to be blocked by the fibers, and the external surface was covered with fibers, as observed from the SEM images (not presented here). The quality of such materials also was found to be considerably inferior to that of PVA-S-BM-CNF, having reduced mechanical strength and larger contact angle, as discussed later. From these results, we conclude that the dispersion of ACF/CNF using a surfactant was critical to producing a superior quality of the film for battery separators. On the other hand, dispersing fibers in the solvent (methanol) used for esterification resulted in agglomeration.

The time of ball-milling for ACF/CNF in the surfactant was found to be critical for uniform incorporation of the fibers within the prepared polymeric film. Relatively longer time (>120 min) of milling produced breakage of the fibers and destruction of its micro-mesopores. On the other hand, shorter time produced relatively longer (~500 nm) and nonuniform dispersion within the film.

3.2. Ionic conductivity

The ionic conductivity measurements were performed on the prepared materials after saturating them with $LiPF_6$ liquid electrolyte. The liquid electrolyte was prepared by mixing equal volumes (5 cm^3) of ethylene carbonate (EC) and dimethyl carbonate (DMC). The calibrated amount of $LiPF_6$ powder was added to the above liquid to prepare 1 M $LiPF_6$ solution [30]. The synthesized separator materials, PVA-M, PVA-S-BM-CNF, and PVA-SL-BM-CNF, were cut into small pieces (10 mm×10 mm) and dipped in the electrolyte at 35 °C for 2 h. The (fabric) samples of ACF/CNF also were cut into the same dimensions and saturated with the electrolyte. After taking out the wet samples, the excess electrolyte was removed by soaking with tissue papers. Some samples were prepared without saturating them with the electrolytes for the comparison purpose. For the measurement of electrical resistance, contacts of thin Cu-wires were made on the prepared film sample by silver soldering. The measurements were made in two ways (types A and B). In type A measurement, the resistance was measured directly across the film, with contacts made on the top and bottom sides of the film. In type B measurement, the contacts were made on the two sides, separated by a distance (the width of the film). The surface resistance of the film was therefore included in type B measurement.

The ionic conductivity was calculated from the measurement of the resistance. The results are presented in Table 1. The data for resistance and conductivity are presented for each sample, with and without being saturated with the electrolyte. All data are reported corresponding to type A measurement, unless and until specified otherwise. As shown in the table, the ionic conductivity of PVA-M is the smallest (1.17×10^{-3} S-cm^{-1}), and that of ACF/CNF is the largest (1.57 S-cm^{-1}). Among all polymeric films, the ionic conductivity of PVA-S-BM-CNF is the largest (1.19×10^{-1} S-cm^{-1}). Thus, the advantage of in situ incorporating ACF/CNF in PVA using a surfactant is obvious. The dispersion of conductive hierarchical carbon web in the polymeric film has caused a remarkable increase (approximately by two orders of magnitude) in the conductivity. The ionic conductivity of the different materials (with or without electrolyte) is in the following order: ACF/CNF > PVA-S-BM-CNF > PVA-SL-BM-CNF > PVA-M. As also observed from the table, the samples prepared by saturating them with the electrolytes had smaller specific resistance and larger ionic conductivity than those prepared without the electrolytes.

To our knowledge, the ionic conductivity (1.19×10^{-1} S-cm^{-1}) of PVA-S-BM-CNF obtained in this study is significantly larger than that in the literature data, for example, larger than 6.76×10^{-4} S-cm^{-1} for the PAN-based separator [31], 1.95×10^{-3} S-cm^{-1} for LLTO/PAN composite fiber [5], 3.1×10^{-5} S-cm^{-1} for the MMA-modified PE separator [6], 3.92×10^{-4} S-cm^{-1} for PVdF/HFP-based separator [32], and 8.90×10^{-4} S-cm^{-1} for PVdF/PE-based separator material [30].

Table 1 also presents the data for PVA-S-BM-CNF, corresponding to type B measurements. As shown, type B measured electrical resistance is more than 1000 times the corresponding resistance obtained by type A measurement. The data have significance. The carbon fibers are embedded within the film. Therefore, the electrical resistance measured by type B measurement includes the significantly large surface resistance of the polymeric film and the small resistance across the film modified by the fibers.

3.3. Contact angle

The contact angle measurements of the PVA-M, PVA-S-BM-CNF, and PVA-SL-BM-CNF films were carried out to ascertain the effects of the incorporated carbon fibers within the polymeric film on the wettability of the electrolyte ($LiPF_6$). The measurements were made for three different samples for each of the four types of films prepared. The contact angles reported in this paper are within ±2°. Fig. 4 shows the images (photographs) of contact angles for different materials prepared in this study, as obtained from the instrument (contact angle goniometer). As per the usual procedure, a drop of electrolyte was deposited on the surface of the material, and the contact angle was immediately measured and recorded. As shown in the figure, the contact angle for PVA-M (Fig. 4A) was measured as 33.3°. The contact angle significantly decreased to 21.1° for PVA-S-BM-CNF (Fig. 4B), indicating significant increase in the wettability of the surface with the electrolyte. On the other hand, the contact angle (26.6°) measured for PVA-SL-BM-CNF (Fig. 4C) was smaller than that for PVA-M but greater than that for PVA-S-BM-CNF. The data re-demonstrate the advantage of using a surfactant for incorporating ACF/CNF within the polymeric film. Interestingly, ACF/CNF was found to be completely wet with the electrolytes. In fact, the drop of the electrolytes immediately dispersed into the surface upon deposition during the measurement. Table 2 summarizes the contact angles measured for different materials. The contact angle for ACF/CNF is listed as approximately zero in the table.

From the data presented in the preceding paragraph, we conclude that PVA-S-BM-CNF synthesized in this study by in situ incorporating the SDS-dispersed ACF/CNF in the film had the smallest contact angle and the maximum wettability with the electrolyte. Approximately zero contact angle of $LiPF_6$ (mixed with EC and DMC) observed on ACF/CNF reflects relatively higher adsorption of the electrolyte by the carbon surface. On the other hand, relatively larger contact angle observed on PVA-M reflects the "phobic" behavior of the surface with the liquid and consequently less adsorption. Further, relatively larger wettability of the carbon surface by the electrolyte may be attributed to the reduction in the effective interfacial surface tension, resulting in the increased adsorption [33].

The use of the surfactant resulted in a uniform dispersion of the ball-milled ACF/CNF within the polymeric matrix, which rendered the PVA film "phillic". Therefore, the contact angle of PVA-S-BM-CNF was measured to be in between that of ACF/CNF and PVA, and greater than that of PVA-SL-BM-CNF. The use of solvent (instead of surfactant) caused agglomeration of the CNF fibers in the latter film and therefore, less adsorption of the electrolyte and increase in the interfacial forces and contact angle.

The smallest contact angle (21.1°) obtained for PVA-S-BM-CNF is comparable with or smaller than those for a few commercial separators: 15.8° for the ionic liquid modified separator, 21.6° for plain separator, 60.9° for Celgard-2320, and 53.1° for Celgard-2730 [34]. For the Li-ion battery, the wettability of the separator by the electrolytes

Table 1
Specific resistance and ionic conductivity of prepared materials.

Sample ID	Without electrolyte			With electrolyte		
	Resistance (Ω)	Specific resistance (Ω-cm)	Ionic conductivity (S-cm^{-1})	Resistance (Ω)	Specific resistance (Ω-cm)	Ionic conductivity (S-cm^{-1})
Type-A measurement						
ACF/CNF	0.05	1.06	9.4×10^{-1}	0.03	6.38×10^{-1}	1.57
PVA-M	3.78	1.51×10^{3}	6.61×10^{-4}	2.140	8.56×10^{2}	1.17×10^{-3}
PVA-SL-BM-CNF	0.085	3.40×10^{1}	2.94×10^{-2}	0.038	1.52×10^{1}	6.58×10^{-2}
PVA-S-BM-CNF	0.079	3.16×10^{1}	3.16×10^{-2}	0.021	8.40	1.19×10^{-1}
Type-B measurement						
PVA-S-BM-CNF	343.000	1.37×10^{5}	7.29×10^{-6}	206.000	8.24×10^{4}	1.21×10^{-5}

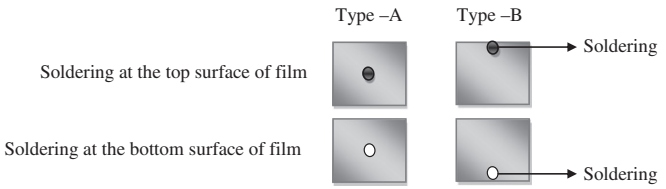

is critical for the battery performance because the separator with good wettability can effectively retain the electrolyte solutions and facilitate the electrolyte ions to diffuse through its pores [1,2].

3.4. Tensile strength as mechanical property

The stress–strain relationship was obtained for evaluating the comparative tensile strength of the prepared films as separator. As per the standard method [35], a rectangular (50 mm × 5 mm) segment of the prepared samples (thickness = 25 μm) was subjected to the initial strain ramp of 0.5 per min and preload force of 0.001 N. The sample temperature was set at 35 °C. The initial distance between the holder grips was set at 20 mm.

Fig. 5 shows the stress–strain curves of different samples plotted from the data. As observed, PVA-S-BM-CNF (the proposed separator material in this study) has the maximum tensile strength when compared with other polymeric materials. The maximum (yield) tensile strength of PVA-M was measured to be 789 kg-f-cm^{-2}. On the other hand, that of ACF/CNF was measured to be expectedly large (2830 kg-f-cm^{-2}). It is obvious that the tensile strength significantly increased (2146 kg-f-cm^{-2}) for PVA-S-BM-CNF, approximately three times larger than that of PVA-M, on incorporating ACF/CNF. The tensile strength of different polymeric samples was in the following order: PVA-S-BM-CNF > PVA-SL-BM-CNF > PVA-M. Also, a sharp increase observed for the tensile strength of ACF/CNF during the load test is the characteristic of carbon fibers, which is different for polymeric materials. The latter materials are gradually stretched (elongated) till the yield stress on increasing load.

The calculated values for the tensile strength of the prepared films are summarized in Table 2. The data emphasize the advantage of incorporating high tensile ACF/CNF within the polymeric film, and in addition, the use of surfactant for dispersing ACF/CNF. The tensile strength (2146 kg-f-cm^{-2}) of PVA-S-BM-CNF obtained in this study may be compared to the same for a few commercial Li-ion battery separators: 1900 kg-f-cm^{-2} for Celgard-2325, 2100 kg-f-cm^{-2} for Celgard-2340, 1500 kg-f-cm^{-2} for Tonen-1 [2], 271 kg-f-cm^{-2} for PVdF-based material [30], and 53 kg-f-cm^{-2}–850 kg-f-cm^{-2} for composite cellulosic separator material [13]. From the presentation of the data in this section, we conclude that the mechanical strength of PVA-S-BM-CNF is superior to most of the commercially available separators and comparable to some.

3.5. FTIR analysis

The FTIR analysis of the prepared samples was carried out to ascertain different functional groups present on the surface and observe their transformation following the in situ incorporation of ACF/CNF in the film during the esterification step. Fig. 6 shows the FTIR spectra of ACF/CNF, PVA-M, and PVA-S-BM-CNF. It may be observed from the figure that there are common characteristic peaks at 3400–3800 cm^{-1}

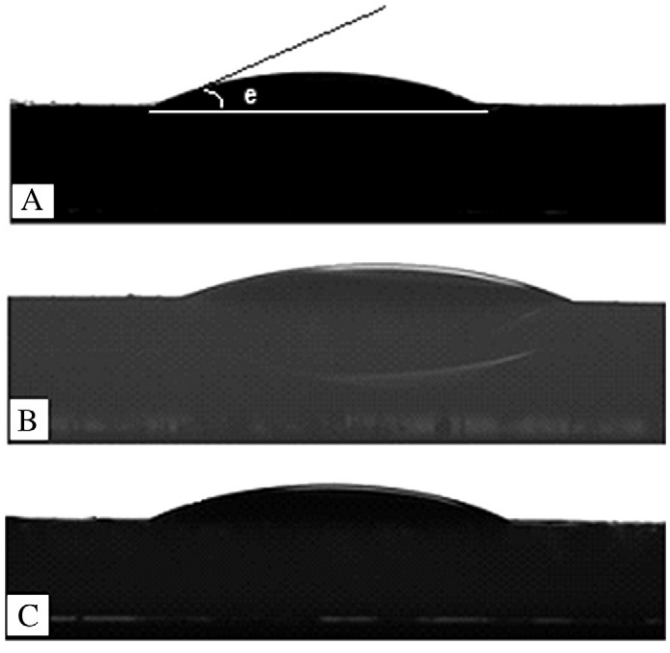

Fig. 4. Contact angle of (A) PVA-M (33.3°), (B) PVA-S-BM-CNF (21.1°), and (C) PVA-SL-BM-CNF (26.9°) films saturated with electrolyte ($LiPF_6$).

Table 2
Contact angle[a] and tensile strength of prepared materials.

Sample ID	Contact angle (degree)	Tensile strength (kgf cm^{-2})
ACF/CNF	Completely wet (~0°)	2830
PVA-M	33.3	789
PVA-SL-BM-CNF	26.9	1599
PVA-S-BM-CNF	21.1	2146

[a] Measured with electrolytes.

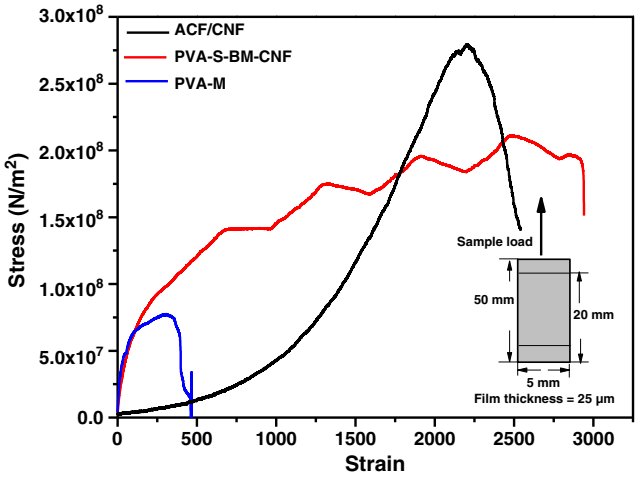

Fig. 5. Tensile strength of ACF/CNF, PVA-M and PVA-S-BM-CNF films.

for all samples. These peaks are attributed to the OH stretching because of the presence of oxygen-containing groups, such as hydroxyl (–OH), phenolic (–OH), and carboxylic acid (–COOH). Such functional groups are inherently present in ACF/CNF [36]. The increased peak-intensity over the range 3400–3800 cm^{-1} for PVA-M is attributed to the hydroxyl groups incorporated during the esterification of PVAc by methanol as well as the modification of PVA with methyl acrylate. The latter reagent along with acrylonitrile was used to increase hydrophobicity of the prepared film. It is important to note that there is no characteristic change observed in the peaks around the wavelength range of 3400–3800 cm^{-1} for PVA-S-BM-CNF, suggesting that the dispersion of the incorporated carbon fibers within the film was essentially physical and the basic chemical characteristic of the prepared material remained intact after the incorporation of the fibers.

The peak observed at ~1685 cm^{-1} for PVA-M is attributed to the C═O stretching of the carboxylic group, which may have arisen from the methyl acrylate monomer cross-liked to PVA. The observed peak of C═O stretching may come from the acetate group also, due to the 92–94% hydrolysis degree of PVA. As per the standard table of characteristic IR absorptions, C═O stretching due to carboxylic and acetate groups occurs over the range of 1760–1690 cm^{-1} and 1760–1665 cm^{-1}, respectively. The characteristic peak observed at ~1020 cm^{-1} is assigned to the C–N stretching because of the acrylonitrile hydrophobic monomer incorporated in PVA-M. The presence of these groups enhanced the absorbability of the electrolyte toward the film. From the figure, no characteristic change in the surface functionality of PVA-S-BM-CNF can be observed, recorroborating the state of the dispersed ACF/CNF within the film being physical.

3.6. DSC analysis

Fig. 7 shows the DSC curves obtained for PVA-M and PVA-S-BM-CNF over the temperature range between 50 °C and 350 °C. For the comparison purpose, DSC analysis also was carried out for ACFs/CNFs, which were in situ incorporated within the polymeric film. There are four salient observations that can be made from the figure: (1) expectedly, there is no (thermal) peak observed for the incorporated ACF/CNF over the entire temperature range considered in the analysis. (2) There is a decrease in the DSC curve for PVA-M and PVA-S-BM-CNF at around 130 °C. Such a behavior (initial decrease in the DSC curve) is the characteristic of PVA and also is observed elsewhere [37]. (3) A relatively minor peak is observed at around 190 °C for both materials, and (4) the major peak is observed at around 275–280 °C for both materials, suggesting the meltdown of the polymeric crystalline phase. The data reflect the potentially high melt integrity and thermal stability of the prepared materials against a catastrophic "thermal runway" condition during the battery operation.

3.7. Physical appearance of the prepared films

Fig. 8 shows the photographs of the different PVA precursor-based films. All films could be easily cut into the desired dimensions using a doctor blade for the laboratory use. The surface of all films visibly appeared smooth, without protrusion of carbon fibers outside the film. Thickness of the films was approximately 25 μm. As shown, PVA-M is yellowish white and partially transparent. The color of PVA-S-BM-CNF is black, as carbon fibers are incorporated in PVA-M. The color of PVA-SL-BM-CNF film, on the other hand, is less black, possibly because of methanol used as a solvent in the reaction medium.

To sum up, the dispersion of ACF/CNF causes significant increase in (a) contact angle, (b) ionic conductivity, and (c) tensile strength of the synthesized PVA film. As shown in the study, ACF/CNF is extremely "phillic" (~0 contact angle) towards the electrolytes and has large ionic conductivity (1.57 S-cm^{-1}) and tensile strength (2830 kg-f-cm^{-2}). It is also thermally stable over a large temperature range. On the

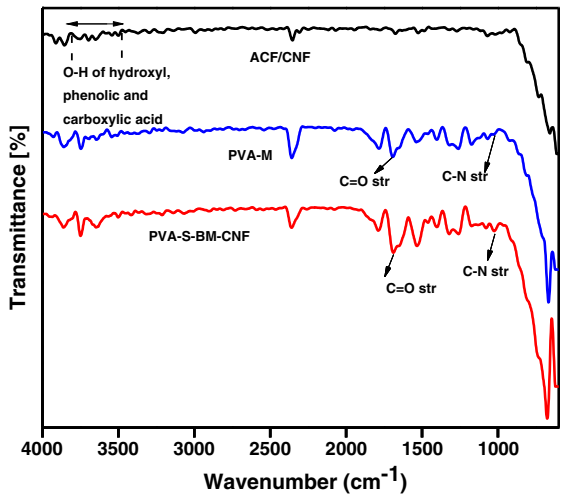

Fig. 6. FTIR spectra of ACF/CNF, PVA-M and PVA-S-BM-CNF films.

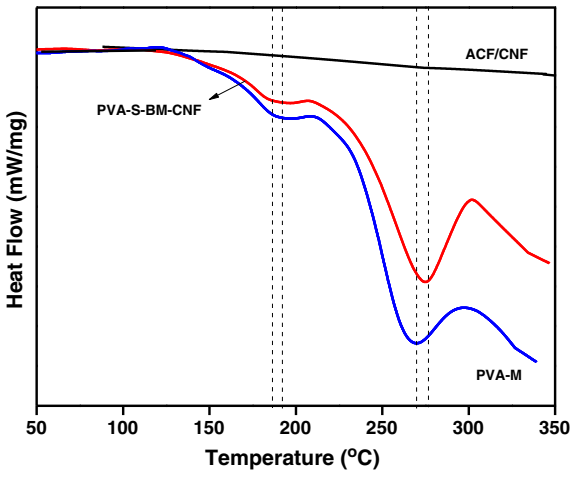

Fig. 7. DSC spectra of ACF/CNF, PVA-M, and PVA-S-BM-CNF films.

Fig. 8. Photographs of prepared PVA-M, PVA-S-BM-CNF, and PVA-SL-BM-CNF films.

other hand, PVA is relatively "phobic", and has smaller ionic conductivity, tensile strength, and less thermally stable than ACF/CNF. Therefore, the dispersion of ACF/CNF within the PVA film results in the enhancement of these properties. The novelty of the present study is to incorporate ACF/CNF within the PVA film, thereby enhancing (tuning) PVA's electrochemical, mechanical, and thermal properties as a separator.

4. Conclusions

In this study, a novel polymeric film (~25 μm) is developed based on the PVA precursor, a relatively low-cost and environmentally benign material, for the potential Li-ion electrolyte battery separators. The film is in situ incorporated (dispersed) with the hierarchal web of ACF/CNF (~500 nm) at the incipience stage of the PVA gel formation. The method to develop such a film also is novel, simple, and economically viable. The synthesized ACF/CNF-dispersed PVA film has significantly large mechanical (tensile) strength (2146 kgf-cm^{-2}), ionic conductivity (0.119 S-cm^{-1}), and electrolyte absorbability (contact angle = 21°) and is thermally stable over a relatively large temperature. This study essentially opens a whole avenue of Li-ion electrolyte battery applications where the hierarchical web of ACF/CNF may be dispersed in situ to a reaction mixture for producing a variety of materials having improved mechanical and electrochemical properties.

Acknowledgments

The authors acknowledge the support of the Department of Science and Technology (DST), New Delhi, for the research grant.

References

[1] P. Arora, Z. Zhang, Chem. Rev. 104 (2004) 4419.
[2] S.S. Zhang, J. Power Sources 164 (2007) 351.
[3] W. Boĕhnstedt, J. Power Sources 95 (2001) 234.
[4] J.Y. Kim, Y. Lee, D.Y. Lim, Electrochim. Acta 54 (2009) 3714.
[5] Y. Liang, L. Ji, B. Guo, Z. Lin, Y. Yao, Y. Li, M. Alcoutlabi, Y. Qiu, X. Zhang, J. Power Sources 196 (2011) 436.
[6] J.H. Park, W. Park, J.H. Kim, D. Ryoo, H.S. Kim, Y.U. Jeong, D.W. Kim, S.Y. Lee, J. Power Sources 196 (2011) 7035.
[7] T.H. Cho, M. Tanaka, H. Onishi, Y. Kondo, T. Nakamura, H. Yamazaki, S. Tanase, T. Sakai, J. Electrochem. Soc. 155 (9) (2008) A699.
[8] J.L. Gineste, G. Pourcelly, J. Membr. Sci. 107 (1995) 155.
[9] S.G. Gwon, J.H. Choi, J.Y. Sohn, S.J. An, Y.E. Ihm, Y.C. Nho, Nucl. Instrum. Methods B 266 (2008) 3387.
[10] K.W. Song, C.K. Kim, J. Membr. Sci. 352 (2010) 239.
[11] J.Y. Lee, Y.M. Lee, B. Bhattacharya, Y.C. Nho, J.K. Park, Electrochim. Acta 54 (2009) 4312.
[12] T.H. Cho, M. Tanaka, H. Ohnishi, Y. Kondo, M. Yoshikazu, T. Nakamura, T. Sakai, J. Power Sources 195 (2010) 4272.
[13] I. Kuribayashi, J. Power Sources 63 (1996) 87.
[14] P.P. Prosini, P. Villano, M. Carewska, Electrochim. Acta 48 (2002) 227.
[15] M. Kim, J.Y. Sohn, Y.C. Nho, J.H. Park, J. Electrochem. Soc. 158 (5) (2011) A511.
[16] A. Subramania, N.T.K. Sundaram, N. Sukumar, J. Power Sources 141 (2005) 188.
[17] D.W. Sheibley, M.A. Manzo, O.D.G. Sanabria, J. Electrochem. Soc. (1983) 255.
[18] W.H. Phillip, L.C. Hsu, D.W. Sheilby, US patent 4154912, 1979.
[19] L.F. Li, US patent 2010/0062342 A1, 2010.
[20] Z. Pan, Z. Deng, R. Li, L. Wang, J. Deng, H. Du, J. Gao, J. Suo, US patent 2010/0178545 A1, 2010.
[21] M.S.P. Shaffer, A.H. Windle, Adv. Mater. 11 (1999) 937.
[22] A.A. Mamedov, N. Kotov, M. Prato, D.M. Guldi, J.P. Wicksted, A. Hirsch, Nat. Mater. 1 (2002) 190.
[23] N. Verma, A. Sharma, Indian patent IPA No. 1157/DEL/2009, 2009.
[24] A.K. Gupta, D. Deva, A. Sharma, N. Verma, Ind. Eng. Chem. Res. 48 (2009) 9697.
[25] M. Bikshapathi, G.N. Mathur, A. Sharma, N. Verma, Ind. Eng. Chem. Res. 50 (2011) 13092.
[26] C.K. Haweel, S.H. Ammar, IJCPE 9 (1) (2008) 15.
[27] Y.M. Lee, J.W. Kim, N.S. Choi, J.A. Lee, W.H. Seol, J.K. Park, J. Power Sources 139 (2005) 235.
[28] Y.K. Lee, J.W. Rhee, W.Y. Cho, J.M. Sung, B.C. Jo, C.H. Lee, I.H. Jung, B.R. Jung, US patent 7435761B2, 2008.
[29] Y.K. Lee, S.H. Park, J.W. Rhee, J.A. Lee, US patent 20090130547A1, 2009.
[30] Y. Huai, J. Gao, Z. Deng, J. Suo, Ionics 16 (2010) 603.
[31] A. Laheäär, H. Kurig, A. Jänes, E. Lust, Electrochim. Acta 54 (2009) 4587.
[32] W. Pu, X. He, L. Wang, Z. Tian, C. Jiang, C. Wan, J. Membr. Sci. 280 (2006) 6.
[33] M. Dhabi, D. Violleau, F. Ghamouss, J. Jacquemin, F.T. Van, D. Lemordant, M. Anouti, Ind. Eng. Chem. Res. 51 (2012) 5240–5245.
[34] C.S. Stefan, D. Lemordant, B.C. Montigny, D. Violleau, J. Power Sources 189 (2009) 1174.
[35] http://www.astm.org 2010, (accessed Aug 2011).
[36] H. Katepalli, M. Bikshapathi, C.S. Sharma, N. Verma, A. Sharma, Chem. Eng. J. 171 (2011) 1194.
[37] V.S. Pshezhetskii, A.A. Rakhnyanskaya, I.M. Gaponenko, Y.E. Nalbandyan, Polym. Sci. 32 (1990) 722.